AFRL-SN-HS-TR- 2002-049

SEMICONDUCTOR SELECTION AND OPTIMIZATION FOR USE IN A LASER INDUCED PULSED PICO-SECOND ELECTROMAGNETIC SOURCE

Dr. Everett E. Crisman
83 Winter Court
Woonsocket RI 02895

FINAL REPORT: MARCH 1998 – SEPTEMBER 1999

APPROVED FOR PUBLIC RELEASE UNLIMITED DISTRIBUTION

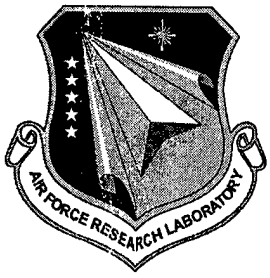

AIR FORCE RESEARCH LABORATORY
Sensors Directorate
80 Scott Dr
Hanscom AFB MA 01731-2909

TITLE: SEMICONDUCTOR SELECTION AND OPTIMIZATION FOR USE IN A LASER INDUCED PULSED PICO-SECOND ELECTROMAGNETIC SOURCE

PUBLICATION REVIEW

This report has been reviewed and is approved for publication.

APPROVED:

Dr John S Derov

John S. Derov
Contract Monitor
Antenna Technology Branch
Electromagnetic Technology Division

FOR THE DIRECTOR

Robert V. McGahan

Robert V. McGahan
Division Technical Advisor
Electromagnetics Technology Division

REPORT DOCUMENTATION PAGE

Form Approved
OMB No. 0704-0188

1. AGENCY USE ONLY *(Leave blank)*	2. REPORT DATE	3. REPORT TYPE AND DATES COVERED
	19 January 2000	Final Report 19 Mar 1998-18 Sep 1999

4. TITLE AND SUBTITLE
Semiconductor Selection and Optimization for Use in A Laser Induced Pulsed Pico-Second Electromagnetic Source

5. FUNDING NUMBERS
F30602-98-C-0019
PE 61102F
PR 2305
TA Be
WU P2

6. AUTHOR(S)
Dr. Everett E. Crisman

7. PERFORMING ORGANIZATION NAME(S) AND ADDRESS(ES)
Dr. Everett E. Crisman
83 Winter Court
Woonsocket RI 02895

8. PERFORMING ORGANIZATION REPORT NUMBER

9. SPONSORING/MONITORING AGENCY NAME(S) AND ADDRESS(ES)
Dr. John S. Derov
AFRL/SNHA
80 Scott Drive
Hanscom AFB MA 01731-2909

10. SPONSORING/MONITORING AGENCY REPORT NUMBER
AFRL-SN-HS-TR-2002-049

11. SUPPLEMENTARY NOTES
Work resulted in one publication: A Two-Element Dielectric Antenna Serially Excited by Optical Wavelength Multiplexing; E.E. Crisman, J.S. Derov, D.D. Lui, P.H. Carr and S.D. Mittleman, Optics Letters, V15,p235 (Feb 1999)

12a. DISTRIBUTION AVAILABILITY STATEMENT
APPROVED FOR PUBLIC RELEASE UNLIMITED DISTRIBUTION

12b. DISTRIBUTION CODE
"A"

13. ABSTRACT *(Maximum 200 words)*

The use of optically induced, d.c. accelerated, semiconductor carriers as a source of picosecond microwave pulses is examined. The purpose of this study was to determine whether 1) phase shifted, multiple (optical) pulses could be generated on a single semiconductor element and 2) whether multiple inline elements could be stimulated with a single optical pulse. Both of the configurations have potential for simultaneously providing the source and phase control necessary for a steerable target recognition array. The efficiency of both technique s are demonstrated in this preliminary study and the gain which could be realized from cooling the semiconductor sources was evaluated for one specimen. Phase differences for multiple pulses were observed and directly related to the special position of the optical pulses with respect to the detector. The cascades sources showed enhanced forward microwave intensity and also an angular dependence consistent with the two sources and detector geometry. Cooling from room temperature to 100K resulted in approximately a three fold improvement in microwave strength (from a single element).

14. SUBJECT TERMS	15. NUMBER OF PAGES
Photonic antenna, reconfigurable antenna, pico-second pulses, gigahertz, pulsed laser, LIPPES	27
	16. PRICE CODE

17. SECURITY CLASSIFICATION OF REPORT	18. SECURITY CLASSIFICATION OF THIS PAGE	19. SECURITY CLASSIFICATION OF ABSTRACT	20. LIMITATION OF ABSTRACT
Unclassified	Unclassified	Unclassified	SAR

ABSTRACT

An analysis has been undertaken to understand the pertinent factors for choosing the semiconductor(s) used to develop a high efficiency, laser, induced, pulsed, picosecond, electromagnetic sources (LIPPES). For this project, the relationship between the laser wavelength and the semiconductor has been studied. Much of the allotted time was spent in preparing the laboratory experimental setup, rebuilding and aligning the lasers used for the experiment and fabricating new specimens for evaluation. With respect to the main thrust of the project, the studies show that: 1) of the specimens on hand, the highest efficiency are generated in material that has a doped epi-layer on a semi-insulating, bulk substrate; 2) the density of states in intrinsic material is too low to permit significant E-M fields to be generated, therefore doped material/epi-layer will be necessary for large field generation; 3) when the laser wavelengths are close to the bandgap of the particular semiconductor the E-M radiation efficiency is significantly increased; 4) the surface density of states and surface activation level plays a significant roll in the efficiency of the device, 5) the application of an antireflection coatings on laser absorbing surfaces of the semiconductor significantly improves the strength of the E-M output; 6) synchronized high voltage pulses, as short as practical, are necessary to minimize the chances of surface breakdown during LIPPES operation.

TABLE OF CONTENTS

SF298	i
ABSTRACT	ii
TABLE OF CONTENTS	iii
LIST OF FIGURES	iv
INTRODUCTION	3
DESCRIPTION OF WORK ACCOMPLISHED	
• YLF Laser Preparation	2
• Ti-Sapphire Laser Preparation	2
• Other Optical Laboratory Facilities	3
• Other Components of the LIPPES Experiment	3
• Specimen and Facilities Preparation	4
• Development of Anti-Reflection Thin Films For Improved Coupling of Laser Energy Into Specimens	5
Background	5
AR Coating Preparation	7
Reflectivity Measurements	8
AR Coating Summary	11
ADDITIONAL ACCOMPLISHMENTS OF THIS PROJECT	11
ACKNOWLEDGMENTS	12
REFERENCE	12
APPENDIX I: (Paper published in OPTICS LETTERS)	13
APPENDIX II: (White Paper on LIPPES Concept)	21
APPENDIX III: (White Paper on Micro-machined MM-Wave Sensors)	25

INTRODUCTION

Some years ago a it was suggested [1] that a wide band microwave source could be generated by using high voltage to accelerate charged carriers that have been optically excited on the surface of a semiconductor. Such sources would have a time domain width controlled by the duration of the optical pulse in combination with the semiconductor, photo-carrier lifetime. Optical excitation could simplify multiple E-M source generation; for example by splitting a single laser beam onto multiple paths. Phase and impedance matching problems, inherent in UHF microwave source - to - antenna coupling, would be significantly reduced with such a scheme. In addition, the E-M sources, as described, would act as their own radiating elements (antennae) thereby producing a compact array, which could be reconfigured electro-optically [2,3] rather than by complex mechanical and/or electronic delay lines schemes. This would be a distinct advantage in the high "g" environments of airborne platforms. Cooling to at least LN_2 temperature would be feasible for airborne applications and has the potential for improving the field strength of such arrays by increasing the mobility and hence the final velocity attained semiconductor photo carriers [6]. Such laser induced, pulsed picosecond electromagnetic sources (LIPPES), have been investigated for some time and the basic concept has be shown to be viable. Research into various aspects of LIPPES has proceeded continuously, albeit at a low level, since 1994. The initial proof of concept was demonstrated by several organizations including Rome Laboratory, Hanscom AFB, MA [4].

The concept, simply stated, is that photo carriers, induced in a semiconductor by an optical laser pulse will accelerate if a quasi-dc electric field is present in the plane of the semiconductor (say between two surface metallic contacts on a thin polished wafer). Such accelerating carriers (generally electrons) will radiate electromagnetic (E-M) fields in proportion to the applied dc field strength up to some maximum velocity controlled by the intrinsic semiconductor parameters; vis-a-vis the mobility. Experimental results of the past two years have generally confirmed this hypothesis and theoretical calculations indicate that the resulting microwave field strength at the surface of the emitter can be as high as the accelerating potential, i.e. in the kilovolt range! The dc field dependence has been examined and reported recently by the Liu, et al. at USAF Rome Lab. Hanscom, MA [5]. In that study, E-M radiation field strength from GaAs and InP were measured as a function of applied dc bias. They demonstrated that, for two candidate materials, a plateau in the radiated field was reached for the dc field above some threshold; about 5.5 kV for GaAs and 12 kV for InP. Based those studies and other information develop thus far, InGaAs should to be an even better source of E-M radiation producing stronger E-M fields at lower dc voltages.

This contract was intended to evaluate the relationships between the wavelength of the excitation laser, the bandgap of the semiconductor and semiconductor surface condition (density of states) on the efficiency of the LIPPES devices. While a complete mapping of the variables was not viable in the short time frame of this project (approximately 73 working days), much useful information was generated that should ultimately lead to a successful application of LIPPES technology to AF needs.

DESCRIPTION OF WORK ACCOMPLISHED

YLF Laser preparation

At the beginning of this project it was recognized that the eight-year-old YLF laser that had the principal excitation source for the majority of the LIPPES experiments was deteriorating and would require some refurbishing. To that end and in parallel with the rest of the program we undertook to completely rebuild and realign the YLF laser. The following main items were successfully completed on the Quantronix YLF laser during the course of this contract:

- The closed cycle, DI water, cooling loop was cleaned and new particle filters were purchased and installed.
- Two new YLF lasing rods with different end configurations were purchased and one was installed in the system. (The original rod had deteriorated to an efficiency of less than 50%.)
- The entire laser, including all mirror surfaces, was cleaned and realigned as per the factory specs.
- The Q-switching section was re-installed and the corresponding output pulses were optimized for power.
- The Pockels Cell, used as the laser peak-pulse selector, was installed in the beam path and optimized.
- The frequency doubling, KDP crystal, section of the YLF system has been install in the optical path and optimizes.
- Re-optimization of the system has resulted in a power efficiency of approximately 95% of the YLF laser at its initial installation.
- Notes and addenda were added to the Quantronix manual so that the alignment can be repeated in the future.

Ti-Sapphire Laser preparation

The Ti-sapphire laser is tunable around the band gap energies of both InP and GaAs. It was essential for this investigation that the Ti-Sapphire laser operate reliably and at peak performance. The system had set unused for the three years prior to the commencement of this project and so significant time was spent realigning and calibrating this laser. Because of difficulties in establishing mode lock operating conditions, Dr. Crisman traveled to the manufacturer home office (Lexel Corp, San Jose, CA) to consult with the experts there. The information attained ultimately allowed us to establish self-mode locking in the femto-second range and active mode locking in the pico-second range (where the experiments were to be performed). The detailed understanding of the Ti-Sapphire laser operation was essential for this and any follow on LIPPES projects. During the course of the contract the following significant items were completed on the Lexel Ti-Sapphire laser:

1. Detailed cleaning and alignment of the Ti-Sapphire Laser has been completed.
2. The laser has been successfully operated with the wavelength selecting, quarter wave plates installed in the optical path.
3. The laser has been successfully operated with the NEOS, electronic mode locking section

installed in the optical path.

4. The alignment procedures for self mode locking were established in the femto-second regime with the 'group velocity delay' optical section in place.
5. Further experiments verified that the active mode locking (using the NEOS system) was functioning properly and that both 76MHz and the 100MHz pulse trains could be established in the pico-second operation regimes.
6. A selection of transmission mirrors was obtained from Lexel so that the various operating modes could be readily established in the future.
7. Finally, the Ti-Sapphire laser was reconfigured to operate in pico-second range and the system was realigned for operation in that mode with active mode locking.
   Once it was determined that the coaxial feedback connection was missing to the NEOS control box, the system regularly operated in the pico-second regime with active mode locking.
8. Notes and addenda were added to the Lexel manual so that the alignment can be repeated in the future.

From 'cold start' the laser can now be placed into pulse mode within approximately 20 minutes. Heretofore the system was not functioning in the pico-second pulse range at all. This laser is now configured so that the semiconductor experiments can go forward.

Other Optical Laboratory Facilities

1. A Spectra Pro 275 monochrometer with CCD detector array was purchased and has been installed on the optics bench with the Ti-sapphire laser. This system is used to determine the precise wavelength of the laser pulses so that the functional dependence of efficiency near the semiconductor band edge can be ascertained.
2. A rapid response photodiode connected to a 250MHz oscilloscope was installed to detect and display the mode lock pulses.
3. Beam splitters were installed so that total power, spectral content and pulse shape could be view simultaneously.
4. The optical benches in the lab have been re-arrange so that the experiments can be integrated on them and a new bench is being installed so that all bench height will be the same.
5. HEPA particle filters have been purchased and installed in the optics laboratory. These have been supplemented with filter paper coverings over the room AC inlets.
6. Work orders have been placed to have the water-to-air heat exchanger for the Quantronix YLF laser replaced by a heat exchanger directly connected to the building's cooling loop. (This is being done to provide more space and reduce noise and vibration in the optics lab.)

Other Components of the LIPPES Experiment

A great deal of attention was also given to evaluating the method of providing the quasi-dc field across the surface of the photoactive specimens. We did a preliminary evaluation with a DC source capable of 10kV maximum voltage. With that source it was determined that above about 300mA, regardless of the voltage, surface leakage and/or current limiting resistor breakdown often caused surface flash-over that was detrimental to the specimens. This is likely due to the I^2R local heating with subsequent run away caused by thermally generated carrier conduction through the

semiconductor surface states abetted by overheating of the one eight Watt, current limiting resistors in the high voltage circuit. This was verified by cooling the surface with expanding dry air spray and noting that the current dc current decreased accordingly.

The original setup had transformer-induced voltage pulse variable up to 20kV, with half width of ten microseconds. Because of difficulties with triggering and synchronization of the HV pulse circuit with the optical pulses, we explored several methods of providing the electric field pulses that could be synced with the Ti-Sapphire, NEOS active mode lock control. To that end we have employed a capacitive discharge, auto ignition system and an automobile spark coil for the HV pulse source. While this was found to provide voltage pulse peaks > 40kV with half widths < 5.0 μs, vulgarities of the internal design of the SCR circuit, used to trigger the discharges, restricted control over the HV pulse amplitudes. We are pursuing the concept by designing our own capacitive discharge system for use with low impedance; automobile high-tension coil designed specifically for transistor ignition systems. When that design is completed, we should be able to reach the 40kV design voltage with pulse widths as short as 1μs.

A 'divide-by' 10^4 digital counter has been designed to facilitate synchronizing the HV pulses with the (100 MHz) optical pulses.

First level automation of the data acquisition, using Lab Windows©, has been completed. This will allow the automated capture of the of the microwave pulse waveforms as a function of various parameters (laser wavelength, optical pulse power, angular position, etc.)

The Tektronix 11802 sampling scope and the Opto-Electronics, Inc. ultra fast, diode detector, which have been the principal components of the synchronization and monitoring systems, both failed during the last quarter of the project. They have been returned to the manufacturer for repair.

Specimen and Facilities Preparation

To a great extent, the success of the proposed material evaluations depended on an accurate knowledge of the semiconductor properties of the LIPPES specimens used for the evaluation. Much remains unknown about the history and properties of the 'old' specimens used here-to-fore for the preliminary studies. We decided early on that we should prepare some 'new' LIPPES specimens, from well-characterized GaAs, so that a reference point could be established against which our measurements could be compared. To that end significant time was expended in 'tuning up' the UHV sputtering system so that its performance would again match the specifications. As part of that phase of the program, we spent some time in calibrating the system by reactively sputtering silicon to form silicon nitride. [This was, also, done to provide etch stop capabilities for one of our other scientist who was fabricating silicon based MEMS structures.] In addition, silicon nitride provided us with the capability of adding anti-reflection coating to the LIPPES specimens for improved efficiency. The results of those experiments are contained below. For the UHV system we accomplished the following upgrades revisions and preparations:

1. A new view port was installed in the UHV deposition system that has allowed a high vacuum of $5x10^{-9}$Torr to be achieved once more.
2. A new cryo-pump was installed.
3. A new ion gage was installed in the UHV main chamber.
4. A procedure was established for fabrication of GaAs LIPPES specimens using our own UHV facilities.
5. The UHV system was used to prepare, GaN, AlN and Si_3N_4 by reactive sputtering.

6. Reactive sputtering of silicon has been incorporated into AFRL/SNHA first successful MEMS device constructions.
7. Specimens of AlN/GaN were prepared in the system and sent for evaluation to X-C Zhang at Rensselaer Polytechnic Institute Physics Department. Prof. Zhang uses a similar generation mode to ours to produce *femto-second* pulses of E-M radiation.
8. The rf monitoring and measurements equipment has been set up and checked out.
9. All the 'old' LIPPES specimens and some of the 'new' specimens (prepared during this project) have been evaluated to establish base lines for our refurbished laser systems.
10. Preparation of more 'new' InP and more new GaAs specimens has begun.

Development Of Anti-Reflection Thin Films For Improved Coupling Of Laser Energy Into Specimens

We developed and evaluate a thin film anti-reflection coating that enhanced the coupling of laser energy into our GaAs LIPPES specimens at specific wavelengths. The layers are of the single index, quarter wave type, matched to specific semiconductor specimens and to laser wavelengths used for optical excitation. The purposes of this development is to increase the laser power coupling into the semiconductor specimens and thereby increase the radiated E-M field strengths of such elements when used as reconfigurable LIPPES sources.

Background: In an earlier program we evaluate the next level of complexity for the LIPPES concept after the original proof-of-principal was established. As part of that evaluation [7], a single source was excited in two spatially separated regions by splitting the exciting laser beam. An alternative configuration was also demonstrated in [7] wherein two specimens, stacked physically in series and biased separately, were excited simultaneously by a (split) laser beam. Near and far field measurements confirmed that a phase relationship could be superimposed on the detector by the opto-mechanical relationship between the source(s) and/or the exciting laser beam(s). That is, by varying the physical position on the surface and/or arrival time of the optical pulses, the angular position of the maximum E-M signal could be controlled. A final configuration, offering promise for further simplification, is shown in figure 1. There, two semiconductors of different band edge absorptions are configures in series and illuminated by a laser which contains TWO wavelength components (viz. a YLF at $\ddot{e}_L$=1.053ìm with a frequency doubled component producing a shorter wave length $\ddot{e}_S$ =0.5265ìm). The shorter wavelength, $\ddot{e}_S$, will be absorbed in the first emitter element (GaAs). The longer wavelength, $\ddot{e}_L$, will pass through the GaAs element but be absorbed in the InP element. Since the E-M pulse from the GaAs travels at essentially the same velocity as the $\ddot{e}_L$ component of the laser pulse, the two arrive simultaneously at the InP and the phase relationship of the E-M pulses from the two sources is preserved.

The results of that study suggested several courses that might be followed in order to increase the E-M signal strength The choice of semiconductor (this project) for instance, was one of the more urgent follow up efforts suggested by that study. The physical layout of the contacts, the profile for the quasi-dc accelerating voltages and the spatial relationships between the semiconductor sources and the light excitation beam where also identified for further study. One parameter that is of utmost importance to all the measurements, now and in the future, is the optical coupling between the light source and the semiconductor. That parameter presents challenges even now at this early stage of evaluation because of the nearly 35% loses at the air/semiconductor interface. Therefore, as part of this study we also did preliminary development of an anti-reflection

coating for one of the semiconductors that are presently the focus of the LIPPES studies.

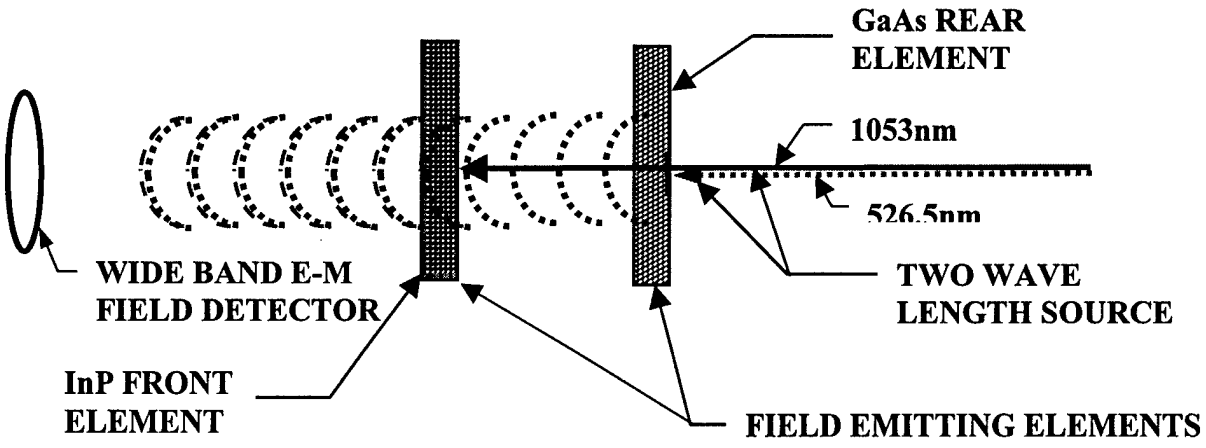

FIGURE 1: LIPPES series configuration for a two 'color' laser source exciting two E-M radiating element in series configuration.

For the experiments performed to date, the light source has been a Q switched, mode locked, frequency doubled, YLF laser with (ML/QS) power of 1.35Watts and pulse energy of approximately 50μJ for 50ps duration pulse. The wavelengths available from the YLF laser are 1053nm and (frequency doubled) 526.5nm. Assuming laser light, at normal incidence, impinging from an air medium onto a non-absorbing, partially reflective, polished surface then the reflectivity, for that single interface condition, is given by the Fresnel reflection equation:

$$\mathbf{R} = \left[\frac{\mathbf{n_S} - \mathbf{n_A}}{\mathbf{n_S} + \mathbf{n_A}}\right]^2 \qquad (1$$

Where $\mathbf{n_A}$ is the index of refraction for the ambient medium (air, $\mathbf{n_A} \approx \mathbf{1}$) and $\mathbf{n_S}$ in the real part of index of the solid (semiconductor). Taking GaAs (the most used semiconductor of these studies thus far) as an example, then $\mathbf{n_S} \approx \mathbf{4.025}$ and the reflection will be 36%! For InP, the other semiconductor use to date, the reflective loses are somewhat less at 31%. Finally, for InSb or InAs, which appear to be an even better E-M sources based on their mobility, reflection lose could be as high as 41%.[1] It is obvious even from these simple estimations that dividing a laser source between many targets will significantly affect the semiconductor excitation level and hence the resulting E-M field strength which is the fundamental gauge for most of the evaluations thus far. Therefore, even a simple AR coating development should reward us with improved absorption and hence increase the precision of the LIPPES research.

[1]The numbers calculated are based on published information for the indicated semiconductors [8, 9, 10] and assume a visible green wavelength of 526.5nm for the YLF laser source after frequency doubling. Some of the variations suggested for improving the E-M field strength will require AR coatings optimized for $\lambda \approx$ 1053nm and other wavelengths near 1000nm.

The salient features of single index antireflection coating have been extensively investigated are the subject of chapters in many textbooks. They will not be reiterated here. The reader is referred to [9] for detailed analysis of the subject. From there, it can be found that the 'best' index for *a single* coating is given by:

$$\mathbf{n_C = (n_A \cdot n_S)^{1/2}} \qquad (2$$

The challenge for GaAs, with $\eta_S \approx 4$ at 526.5nm, was to specify and deposit a dielectric that, 1) would have an index variable about 2.00 ± 0.10, 2) will withstand the humidity and common solvent fumes of the laboratory and 3) can be formed into sputtering targets from available high purity chemicals.[1] For example at 526.5nm the simple calculation of equation (2 above would indicate an AR coating with index on the order of '2' for GaAs. From various published sources, some AR candidates can then be defined. For example, Si_3N_4 has $\mathbf{n_C = 1.97}$ **to 2.02,** when deposited by sputtering, and is readily available in very high purity. There is tabulated information on a variety of dielectric compounds for which the refractive index has been measured at least over some portion of the visible and near infrared spectrum [9, 10]. It is also possible to 'tailor' a coating for a specific index values. Ternary mixtures such as silicon oxynitride, SiO_xN_y, with **1.46 (SiO_2)** $\leq \mathbf{n_C} \leq$ **2.10 (Si_3N_4)** and aluminum oxynitride, AlO_xN_y with **1.76 (Al_2O_3)** $\leq \mathbf{n_C} \leq$ **2.2(AlN)** would provide a composition tunable index of high durability (hardness and moisture resistance).

AR Coating Preparation:

All films were prepared by reactive rf magnetron sputtering in a S-steel chamber pre-cryo-pumped (15 °K, closed cycle He) to a pressure $P < 5x10^{-8}$ Torr. After the specimens were introduced into the vacuum chamber and prior to introduction of the sputtering gases, the system was baked to T > 100°C to reduce the residual oxygen/hydroxyl partial pressures. Approximately 12 hrs was required for the bake-out cycle. Zero grade argon and nitrogen were introduced through PID gas flow controller and associated valves. Total pressure for the film production was 5mT for the combined Ar+N_2 gases (typically 4mT Ar and 1mT N_2 during the sputtering cycle). The target for all the runs of this study was polished, N-type semiconductor grade, silicon wafers doped to $1x10^{16}$ with phosphorous. The specimens where nominally cleaned by rinsing in acetone and/or methanol and blown dry with N_2 before loading into the UHV chamber. The target to specimen distance was 18cm. All run were done with total RF power at 200 Watts.

In order to develop a baseline for sputtered Si_3N_4 thickness, calibration runs were done with silicon wafers (rather than GaAs) as the substrate specimens. Typically three runs were done before the silicon *target* was changed (to prevent 'sputter-through' of the target). The data in figure 2 shows the effect of the N_2 partial pressure on the silicon deposition rate. As anticipated, there is an inverse relationship of deposited rate with increasing partial pressure of N_2 (in Ar).

---

[2]It should be noted that the added flexibility provided by double layer AR coating can almost certainly provide $R \approx 0$ for single wavelength sources at normal incidence [9]. Since double layering allows both thickness and index of the AR films to be varied, it is possible to choose for the interface AR layer a surface-passivating compound. Surface passivation will allow the dc bias field to be increased as necessary to insure velocity of saturation of the accelerated charges. So, this research also provides an excellent foundation for future efforts to optimize the LIPPES technique for airborne and other applications.

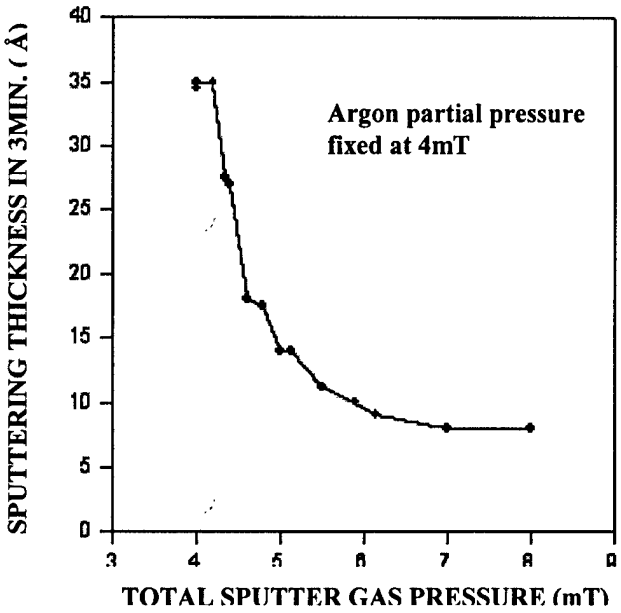

FIGURE 2:
Effect of N2 partial pressure on the silicon sputtering rate as a function of total pressure for Ar alone and Ar plus N_2 for a fix, 4mT, Ar component.

Reflectivity Measurements:

Evaluation of the Si_3N_4 films as AR coatings was performed by measuring the reflectivity directly as a function of wavelength using our LEXEL, model 480, Ti- Sapphire laser excited by a 5 Watt, cw, SPECTRA PHYSICS, Millennia, diode pumped, YAG laser (frequency doubled to 532nm). The LEXEL was fitted with dielectric cavity mirrors optimized for a wavelength range of $700 < \lambda < 850$ nm and was wavelength tunable via a rotating bi-refringent crystal. A dielectric mirror reflected 5% of the extant light into a NEW FOCUS, Inc. Model 7711 Fuzeau wavelength meter used to monitor the λ parameter. Approximately 8% of the remaining power was reflected, with a microscope slide, to the detector element of an OPHIR Laser Power Meter used to monitor the incident power.[2] The remaining light passed through the slide and, after reflecting form the specimen under test, was incident on a MOLECTRON EPM1000 energy/power meter fitted with a J3 detector. A program was developed using HP-VEE to acquire data from the individual measuring devices.

The procedure for obtaining the data was to adjust the bi-refringent crystal for a specific wavelength and then run the program, which took ten readings for each of the λ settings. The data was stored in tabular form and later averaged to provide incident power, reflected power and reflectivity ($P_{reflected}/P_{incident}$) as a function of λ for the plots below.

Before each specimen was measured, a first surface mirror was placed at the specimen position, the two power meters were 'zeroed' with the laser blocked and the room lights off, and then the laser was turned on and the ratio of incident to reflected power was measured. This number was then use as the '100% reflectivity' value for adjusting the subsequent measurements with the specimen in place.

[3] The m ope slide had essentially 'flat' transmission over the λ range used here and so no correction was made for its prese

Prior to evaluating the AR coated specimens, the reflectivity setup, described above, was used to measure a specimen of un-coated GaAs of the type that was intended for subsequent AR coating. This was done after the GaAs was successively cleaning in e-grade acetone, e-grade methanol, etched in HF:NH_3OH, rinsing in DI-water and finally blow drying in dried zero grade nitrogen. The specimen was measured as described above and then the plot of reflectivity versus wavelength was generated as shown in figure 3.

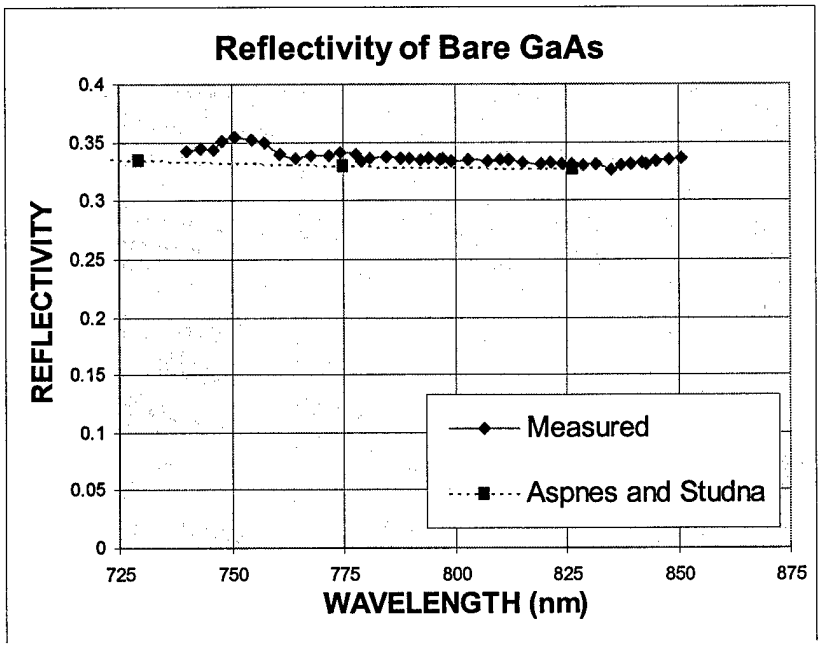

FIGURE 3: Comparison of reflectivity of GaAs, as measured for these studies with reported data from the literature[8].

Added to that plot is the data of Aspenes and Studa [8] which was made on vacuum cleaved GaAs at $1x10^{-9}$T and is the most accurate available for GaAs. As can be seen in the figure, the data for this study tracks well the published data except for small variations in the region around 750nm. Based on the good agreement here the measurement system was applied to the AR coated specimen in the same fashion.

The plot of figure 4 shows the reflectivity of the 167nm-coated specimen (#5239). The 167nm AR coating was prepared primarily as a thick layer on the first GaAs specimen for reference purposes. When it was measured for reflectivity, it was found to approach a reflection minimum at 760nm. This is in agreement with the predicted minimum λ for a film of 167nm thickness, which should occur at an odd multiple of $1/4\lambda_C$, i.e. the wavelength corrected for the index of the AR coating (in this case N=17 would imply a minimum for 161nm thickness). As seen in the figure the reflectivity not only is approaching a minimum but also has an extremely low absolute reflectivity on the order of 0.5%! This means that thicker layers are acceptable and might even have some advantages over the first quarter λ thickness due to better adhesion.

There are two separate series of data plotted in figure 4. Series 1 was done with the small amount of 532nm light that 'bleeds through' the optical path and originates from the diode/YAG laser used to excite the LEXEL Ti-Sapphire system. The series 2 data was a re-run of the same #5329 specimen done after filters had been added to remove that 532nm component. As can be

seen, the reflectivity is further reduced when the stray background component is removed.

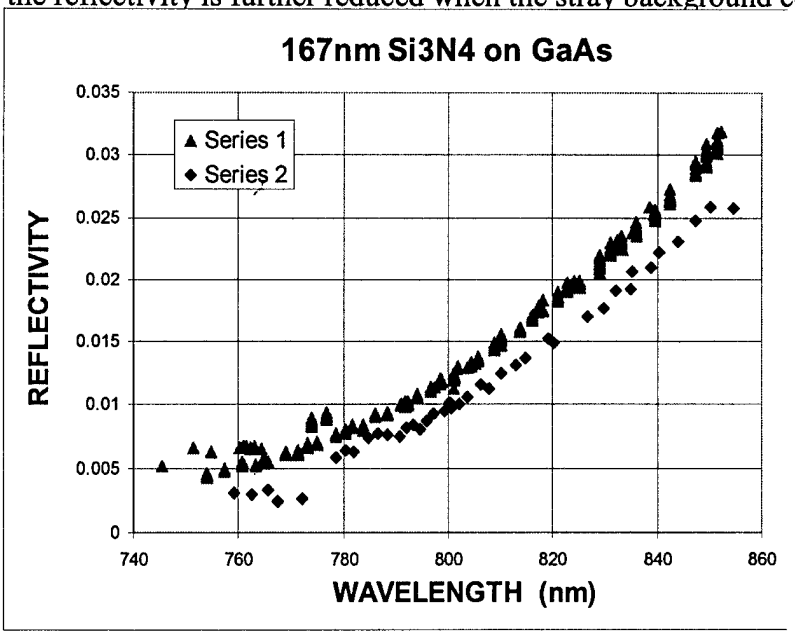

FIGURE 4: Wavelength dependence of Si_3N_4 films reactively sputtered on to GaAs specimen #5239: Series 1 with Ti-Sapphire plus 532 nm YAG component present, Series 2, with 532 nm component removed.

Of the three remaining specimens listed in the table above, #5241a was not measured because the film had clearly delaminated for the GaAs substrate leaving a mottled surface appearance.

AR coating 5421b had a design thickness of 64.9 nm chosen to minimize reflection at 526.5nm which is $\lambda/2$ of one of the laser lines intended for use as in the LIPPES system. The incident and reflected power data and the resultant reflectivity are plotted for that specimen in figure 5. A polynomial curve fit is has been added for the reflectivity data. Extrapolation of that equation to shorter wavelengths gives a minimum reflectivity at 670nm, about a 21% error, but with an absolute reflectivity on the order of 5%.

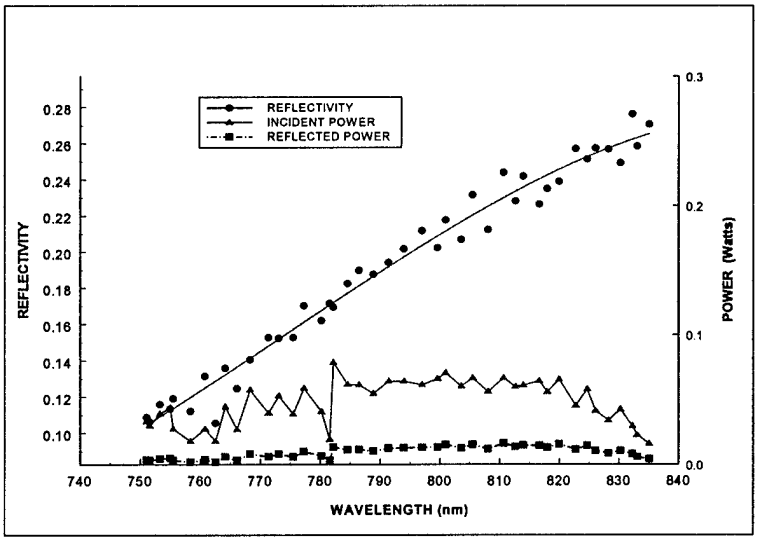

FIGURE 5: Reflectivity versus wavelength for specimen #2541b with 64nm AR coating. Specimen optimized for minimum λ reflectivity at 526.5 nm. ($\lambda/2$ of the 1053nm YLF laser used for LIPPES experiments).

A similar plot is shown in figure 6 for AR coating #5242 with a 97.6 nm design

thickness. Here again the original incident and reflected powers are plotted along with the resulting ratio (P_i/P_r) to give the reflectivity. The polynomial curve fit for that curve appears to be approaching a minimum in the vicinity of 850 nm, which implies an error on the order of 6%. Since leveling off of the curve is not observed here the error is likely greater but the reflectivity at minimum will clearly be less than 10% at the minimum. The main source of disagreement between the predicted minima and that indicated by the data is probably the relatively large area covered by the reflectivity probe beam. This allows the sampling of areas were there is gradients in the thickness and hence variations in the reflectivity values. Time constraints did not permit the investigation of that explanation, but experiments are continuing at the AF laboratory to evaluate the effect. In general we have shown that Si_3N_4 reactively sputtered films can be varied in thickness to provide reasonable matches to specific wavelengths. Refinements of this process should provide repeatability to within a few percent in λ with minima in reflectivity loses less than 5%.

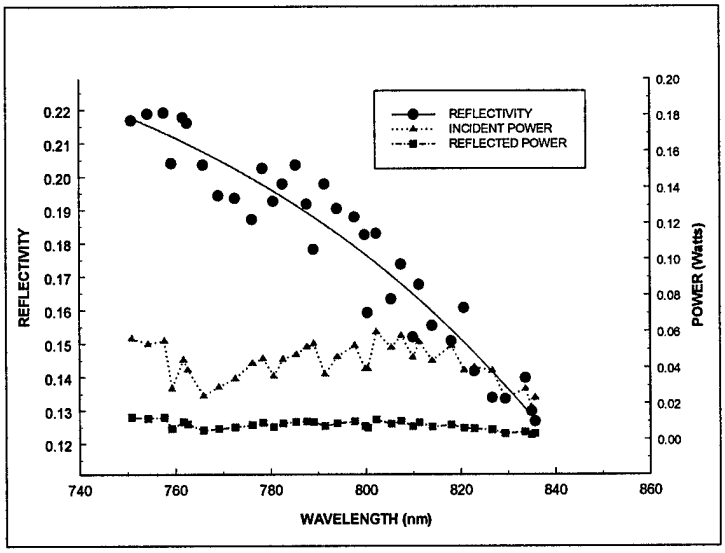

FIGURE 6:
Reflectivity versus wavelength for specimen #5242, with 97.6nm AR coating. Specimen optimized for minimum λ reflectivity at 800 nm.

AR Coating Summary:

We have developed a procedure for reactively sputtering continuous Si_3N_4 thin film anti reflection coating onto GaAs for the purpose of enhancing the transmission of discrete laser wavelengths. Independent measurements of absolute reflectivity show that those AR coatings reduce the reflective losses to < 5% and that the process control is sufficiently precise to allow the film thickness to be controlled to within ±10nm.

ADDITIONAL ACCOMPLISHMENTS OF THIS PROJECT

- The paper accepted for publication in Applied Optics Letters during the third reporting period has been published. It is included as Appendix I of this final report.
- We have prepared two white papers, describing aspects of the LIPPES concept, and aspects of MEMS switch construction for submission to AFOSR and DARPA. Theses are included as Appendices II and III of this final report.

ACKNOWLEDGEMENTS

I wish to particularly thank Dr. John Derov and Capt. J. R. Reid, (Ph.D.), of AFRL/SNHA for the many hours of constructive discussions, physical labor and general support that they provided during the course of this project.

REFERENCES

1. Ch. Fattinger and D. Grischkowsky, **Tetrahertz Beams,** *Appl. Phys. Lett.,* Vol. 54, pp 490 - 492, (1989).
2. B .B. Hu a. t. Darrow, X. -C. Zhang and D. H. Auston, **Optically Steerable Photoconducting Antennas,** *Appl. Phys. Lett.*, Vol 56, No. 10, pp. 886 - 888, (1991).
3. X. -C. Zhang and D. H. Auston, **Generation of Steerable Submillimeter Waves from Semiconductor Surfaces by Spatial Light Modulators,** *Appl. Phys. Lett.*, Vol. 59, pp. 768- -770 (1990)
4. D. W. Liu, J. B. Thaxter and D. F. Bliss, **Gigahertz Planar Photoconducting Antenna Activated by Picosecond Optical Pulses,** *Optics Letters,* Vol. 15, No. 14, pp. 1544 - 1546 (July, 1995).
5. W. Liu, P. H. Carr and J. B. Thaxter, **Nonlinear Photoconductivity Characteristics of Antenna Activated by 80 - Picosecond Optical Pulses**, *IEEE Photonics Technology Letters*, Vol. 8, No. 6 (June, 1996).
6. E. E. Crisman, **Evaluation Of Semiconductor Configurations As Sources For Optically Induced Microwave Pulses,** Final Report to AFOSR 1996 Summer Faculty Research Program, to be published (Dec., 1996)
7. D. W. Liu, E. E. Crisman, J. S. Derov, P. H. Carr and S. D. Mittleman, **Two and Three Dimensional Reconfigurable Arrays Using Optical Generation in Semiconductors as the Source -Antenna Elements,** presented at *The 7th Annual DARPA Symposium on Photonic Systems for Antenna Applications (PSAA-7),* Monterey, CA, (January, 1997)
8. D. E. Aspenes and A. A. Studna, **Dielectric Functions and Optical Parameters of Si, Ge, GaP, GaAs, GaSb, InP, InAs, and InSb from 1.5 to 6.0 eV,** *Phys. Rev. B*, Vol 27, No. 2, pp. 985-1007, (1983).
9. ***THIN FILM OPTICAL FILTERS***, by H. A. Macleod, Macmillian, New York NY, 2nd ed., pp 78 - 86 (1986).
10. See for example, ***CRC Handbook of Laser Science and Technology, Supplement 2: Optical Materials,*** M. J. Weber editor, CRC Press, pp. 30 - 64. (1995).

Appendix I

(Paper Published in *OPTICS LETTERS*)

A Two-Element Dielectric Antenna Serially Excited by Optical Wavelength Multiplexing

E. E. Crisman*, J. S. Derov, P. H. Carr, and S. D. Mittleman

Air Force Research Laboratory

Electromagnetics Technology Division (AFRL/SNHA)

Hanscom AFB, MA 01731-3010

617-377-4038 voice, -1074 FAX

mittleman@maxwell.rl.plh.af.mil

D. D.-W. Liu

Sanders- A Lockheed Martin Company

Advanced Technology Division

P.O. Box 868, MER 24-1583

Nashua, NH 03061

keywords: photoconductive antenna, bandgap energy, nonlinear photoconductivity, threshold bias field, pulsed picosecond lasers, wavelength division multiplexing, microwave.

* Dept. of Physics, Box 1843, Brown University., Providence, RI 02912

Published in *OPTICS LETTERS*, **V15**, p235 (February, 1999)

ABSTRACT

A single, pulsed, laser beam containing multiple wavelengths (wavelength multiplexing) is employed to activate two semiconductor antennas in series. The dielectric nature of the semiconductors permits serial cascading of the antenna elements. Recently observed nonlinear characteristics of radiated field as a function of the free carrier accelerating (bias) voltage are use to minimize the small interactions between elements. We demonstrate that the temporal EM radiation distribution of two serial antennas is sensitive to the three dimensional pattern of the optical excitation source. This, in turn, can be varied continuously by optical means to provide reconfiguration of the array.

In this letter we report the performance of *two* photoconductive antenna elements excited in series by picosecond laser pulses. Rather than provide separate optical pathway to each element, two wavelengths are entrained in a single optical beam. This results in a more compact antenna array. Each semiconductor element is tailored to respond to only one of those wavelengths. Such an array can be re-configured by the wavelength content of the optical beam. When combined with co-planar excitations (multiple excitations of the same element), three-dimensional electromagnetic (EM) source antennas are readily achieved.

Because of their large bandwidth, pulsed microwave sources, operating in the gigahertz range, have been suggested for a number of applications; as ground penetrating radar (anti-personnel mine identification, utilities location) remote triggering encoders in mining, automobile anti-collision systems, aircraft type identification portable medical and security scanning, to name a few.[1] The use of semiconductor radiating elements combined with diode lasers and laptop size computers should result in compact, portable units as compared with systems in use today.[2] Such configuration do not require the microwave 'plumbing' and mechanical steering associated with conventional centimeter wavelength sources and antennae.

Lasers, (operating in either the CW or pulse modes,) activate the semiconductor elements by generating free carriers[3-6]. Those photo-carriers are accelerated in an externally applied electric field to produce EM radiation. When not illuminated, the semiconductor elements are essentially transparent to high frequency EM fields and, therefore, are not interactive with other components. Because of their dielectric nature, inactive semiconductor elements also have a lower microwave cross section then their metallic counterparts.

The concept and general experimental setup of the laser induced, pulsed, picosecond, EM sources (LIPPES) have been described in detail elsewhere[5]. Briefly, a mode-locked, Q-switched YLF laser system provides 50μJ pulse energy with 80ps pulse duration at a wavelength of 1053nm. The laser pulses are selectively chosen, by a Pockel, cell at a repetition rate of 378Hz, and a KDP frequency doubler converts the pulses to a wavelength of 527nm. The doubling is accomplished in such a manner as to allow a significant amount of energy to radiate at 1053nm as well. An photo-detector is used to trigger a TEK11802 sampling scope. Pulses of 100ps duration are readily resolved and 10ps resolution is possible with this setup. A 20kV, 5μs, bias pulse is synchronized with the laser pulse. Pulsed bias is use instead of DC bias to reduce heating and surface flash over on the elements. Fig. 1 illustrates a serial configuration of the photoconductive array of two semiconductor elements photo-activated by such a dual wavelength laser source.

The two-element system consists of GaAs wafer in the rear and InP wafer in front. Undoped GaAs (bandgap Eg=1.43eV @ RT) strongly absorbs the 526nm but is transparent at 1053nm wavelength, while the InP with Fe impurities (Eg=1.32eV @ RT), absorbs strongly at 1053nm. As a result, in-line array

elements are activated. For optimization, the absorption edge and thus the wavelength sensitivities of the semiconductors can be adjusted by varying the density and species of the impurities.

The nonlinear characteristics of the radiated field versus the bias field, generated by a gigahertz photoconducting antenna, have been reported elsewhere[7]. The amplitude of such fields, E(t), is proportional to their final velocity (v), as described in the following equation:

$$E(t) \propto \frac{ev(1-R)}{\hbar\omega} \int_{-\infty}^{t} dt' I_{op}(t') \exp[\frac{(t-t')}{\tau_r}] \qquad (1)$$

where **e** is the unit charge quantity, ***v*** is the carrier velocity, ***R*** is the optical reflectivity of the semiconductor at frequency ω, $e\nu$ is the photon energy, I_{op} is the optical intensity, and τ_r is the photo-carrier lifetime.

Typically, the accelerating carriers (usually electrons) in the semiconductor can reach their final velocity within a few picoseconds or less, i.e. a time much shorter than the optical pulse duration of about 80ps. Consequently, the waveform of the generated microwave pulse emulates the profile of the optical pulse in the time domain. The carrier velocity is not linear with the bias electric field, and some threshold value exists above which a saturation plateau is observed[7]. This relationship is shown in Fig. 2.

With the bias field is set at the plateau, the photo-induced EM signal will become insensitive to variations of the bias field. Taking advantage of this property, the bias field of the front element was established above the threshold value for InP (6kV/cm for GaAs, and 12kV/cm for InP). Therefore, the EM field arriving from the rear (GaAs) element did not affect the generation of EM field in the front (InP) element (see Fig. 3). Furthermore, the EM pulse and the optical pulse will arrive essentially simultaneously at the front element thus ensuring that the combined (front and rear element) EM field will be in phase. In this configuration, the couplings between the elements are expected to be minimal, and the total radiation signal in the far field is given as the superposition of the individual EM fields. Higher gain and beam width narrowing of the far field EM radiation is thus expected.[8,9] This was confirmed experimentally, as shown in Fig. 4. Note in that figure that the pattern from the combined elements is approaching the cosine-squared shape while the single element pattern is significantly broader. This is consistent with dipole versus monopole behavior. The final velocity of free carriers in III-V semiconductors decreases with electric field above some threshold[10]. Such "negative differential conductivity" behavior is applicable to photo-carriers as well[11] and can be used to further reduce inter-element coupling. By taking advantage of the fact that the microwave signal has the opposite polarity as the bias field[12], the electromagnetic pulse from the rear element, arriving at the front element will decrease the bias field there. Referring to Fig. 3, if the bias on the front element is to the right of the plateau, *decreasing* the bias will actually *increase* the carrier velocity. Note finally that the direction of far field maximum amplitude aligns with the optical beam direction permitting the EM pulse to be steered optically.

It is important to note that the power that might be realized from LIPPES devices is relatively independent of the laser power provided there is sufficient fluence to ensure that all of the illuminated semiconductor volume is saturated. We have estimated[5] individual peak powers of 1kW (a conversion of the static electric energy, $\varepsilon E^2/2$, stored in a 10 square centimeter photoconducting antenna area with a typical 1 μm optical absorption depth for a 50 ps pulse). From our measurements of radiated field strength, at a distance of two meters, it was clear that the field was much less that the 1kV estimated. This can be attributed to the fact that the field electrode configuration was not optimized and that the laser power was insufficient in these initial trials to achieve saturation fluence. Also, the total radiated power should increase as the square of the number elements.

In summary, we have demonstrated, for the first time that two photocónductive antenna elements can be optically excited in a in-line serial configuration with a single laser source. The array elements are controlled and reconfigured by optical wavelength multiplexing. Mutual couplings or cross-talk among the elements was reduced by setting the bias fields at the plateau voltages for the individual semiconductor sources. The radiation beam directionality as well as its intensity can be manipulated via a fiber optical network and choice of input optical powers.

ACKNOWLEDGMENTS

The authors are grateful for the helpful discussions of J. B. Thaxter at Rome Laboratory, A. J. Devaney, and E. A. Morengo at Northeastern University. Support for co-author E. E. Crisman, was provided by Air Force Office of Scientific Research and the Department of Physics at Brown University.

REFERENCES

(1) Roland A. Gilbert, and Gerald T. Pirrung, "Structurally-embedded reconfigurable antenna technology", in Proceedings of the Sixth Annual ARPA Symposium on Photonic System for Antenna Applications (1996),

(2) H. Zmuda and E. N. Toughlian, Photonic Aspects of Modern Radar, Boston: Artech House (1994).

(3) Ch. Fattinger, and D. Grischkowsky, "Terahertz beams", Appl. Phys. Lett., Vol. 54, pp. 490-492 (1989).

(4) X.-C. Zhang, and D. H. Auston, "Generation of steerable sub millimeter waves from semiconductor surfaces by spatial light modulators", Appl. Phys. Lett., Vol. 59, pp. 768-770 (1991).

(5) D. W. Liu, J. B. Thaxter, and D. F. Bliss, "Gigahertz planar photoconducting antenna activated by picosecond optical pulses", Opt. Lett., Vol. 20, pp. 1544-1546 (1995).

(6) David Liu, Dave Charette, Marcel Bergeron, Henry Karwacki, Stephen Adams, and Bruce Lanning, "Structurally- embedded photoconductive silicon bow tie antenna", IEEE Photonics Tech. Lett. Vol. 10, 716-718 (1998).

(7) D. W. Liu, P. H. Carr, and J. B. Thaxter, "Nonlinear photoconductivity characteristics of antenna activated by 80-picosecond optical pulses", IEEE Photonics Tech. Lett. Vol. 8, 815-817 (1996).

(8) E. Marengo, A.J. Devaney and E. Heyman, ``Analysis and characterization of ultrawideband and scalar volume sources and the fields they radiate," IEEE Transactions on Antennas and Propagation Vol. AP-45, pp.1098-1106, 1997

(9) E. Marengo, A.J. Devaney and E. Heyman, ```Analysis and characterization of ultrawideband scalar volume sources and the fields they radiate: Part II, "IEEE Transactions on Antennas and Propagation Vol. AP-46, pp.243--250, 1997

(10) S. M. Sze, Physics of Semiconductor Devices, 2nd ed. (Wiley, New York, 1981), pp. 638-651.

(11) G. M. Wysin, D. L. Smith, and A. Redondo, "Picosecond response of photo excited GaAs in a uniform electric field by Monte Carlo dynamics", Phys. Rev. B, Vol. 38, pp. 12514-12524 (1988).

(12) J. T. Darrow, X.-C. Zhang, D. H. Auston, and J. D. Morse, "Saturation properties of large-aperture photoconducting antennas, IEEE J. Quantum Electron. Vol. 28, pp. 1607-1616 (1992)

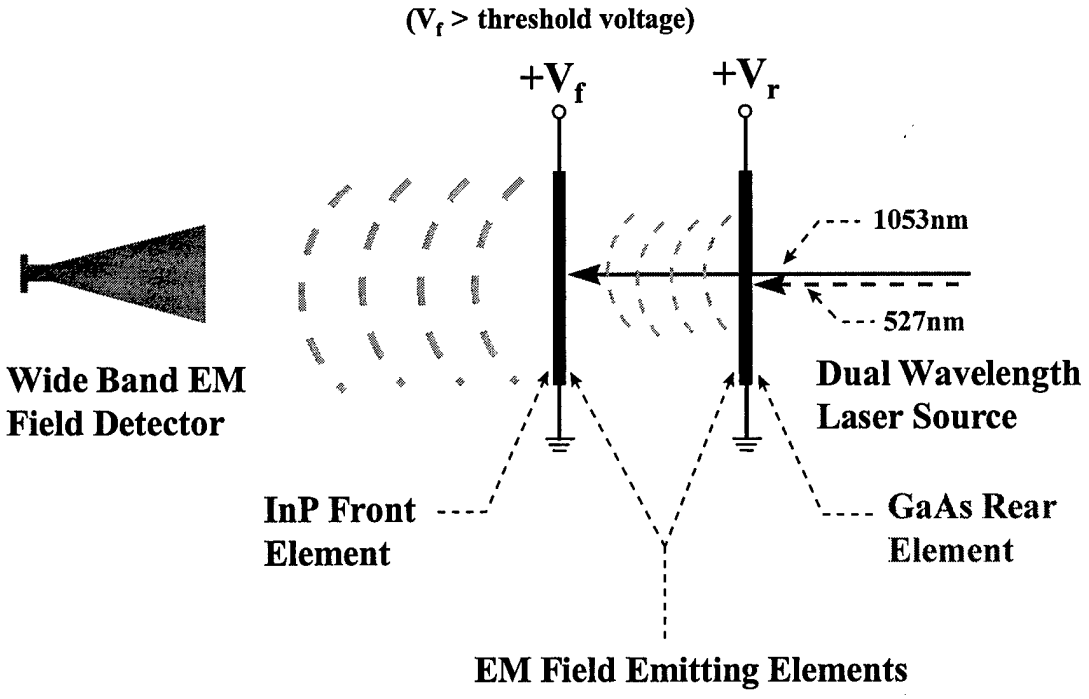

Fig. 1: LIPPES series configuration for two 'color' laser source exciting two EM radiating elements.

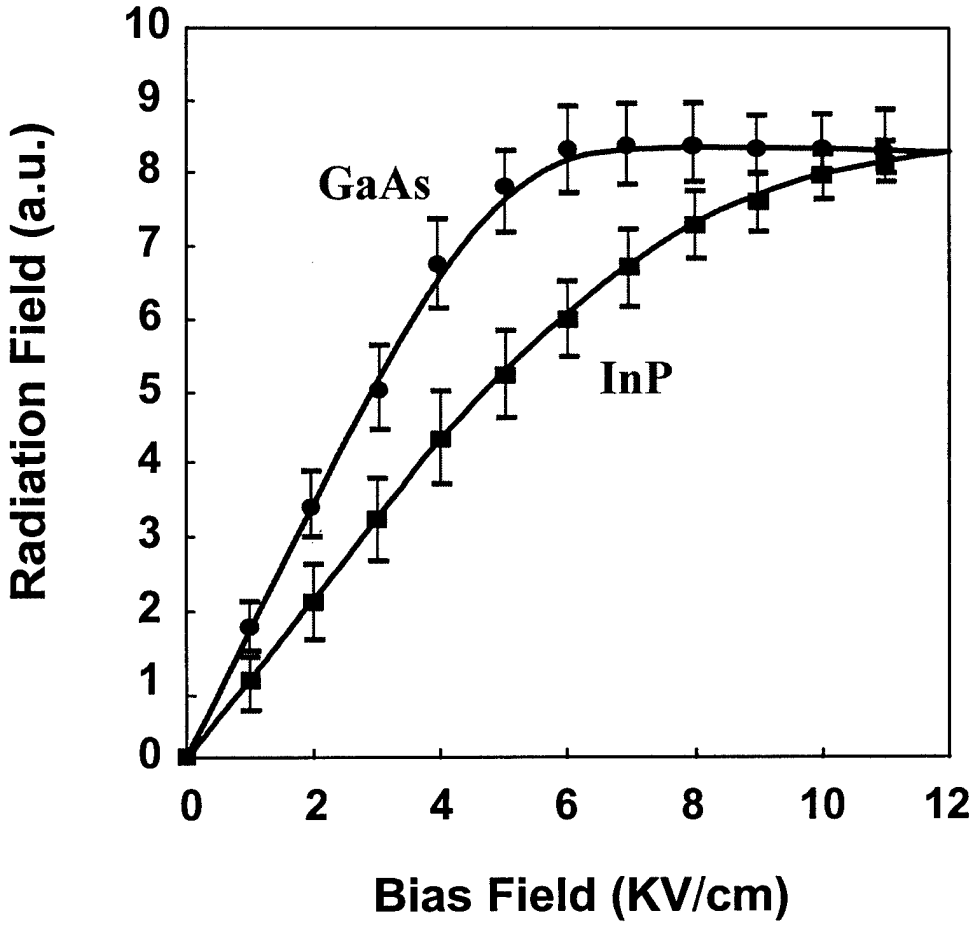

Fig. 2: EM field amplitude as a function of the bias field for GaAs, and InP with the optical fluence at 0.3J/cm^2. The two curves are scaled to have a same radiation field magnitude at the bias field of 12 kV/cm (After Ref. 7 by Liu, Carr, and Thaxter).

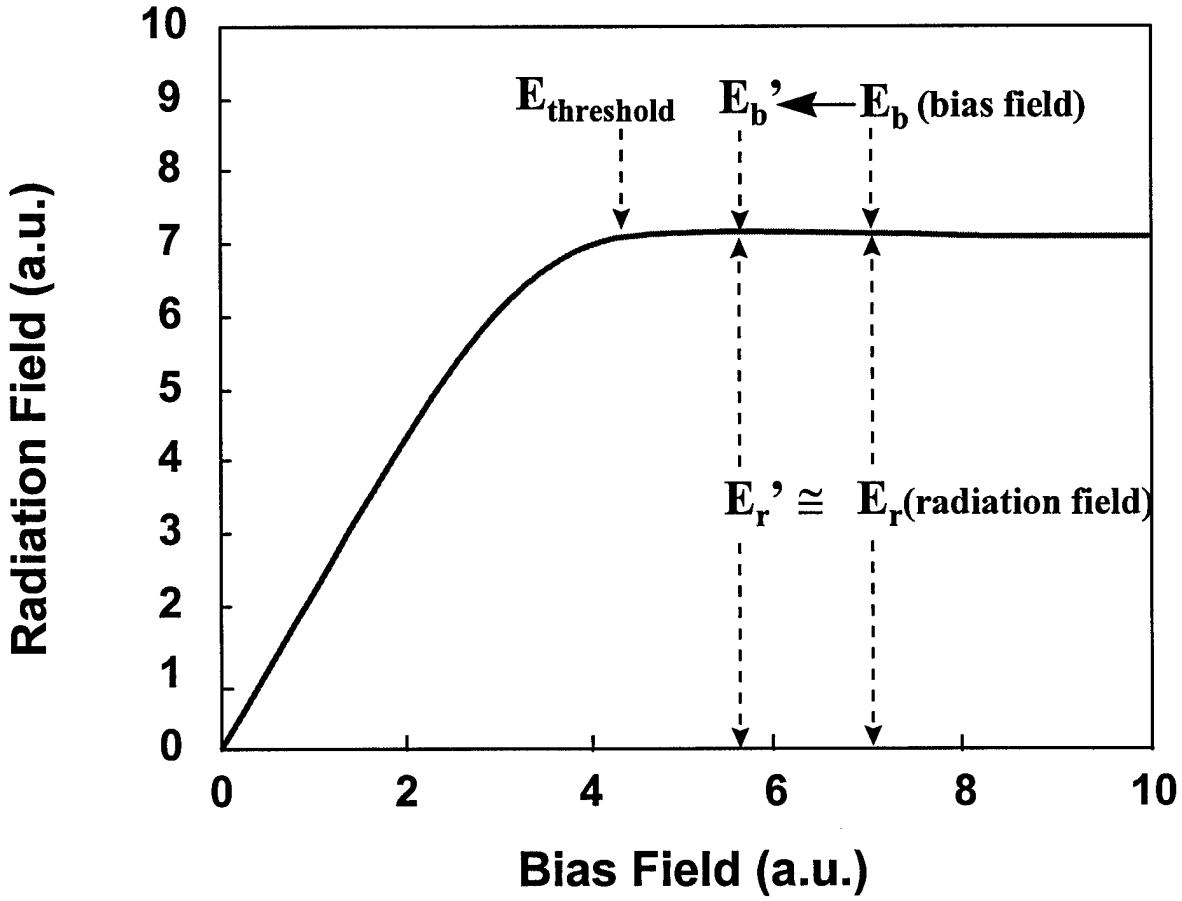

Fig. 3: Typical nonlinear behavior of the radiation power versus the bias field for III-V photoconductive antenna. The shift of the actual bias field from Eb to Eb' due to other arrived EM pulses will give only insignificant disturbance since Er' (radiation field) is nearly equal to Er. Thus, the coupling among the photoconductive antenna elements is minimal.

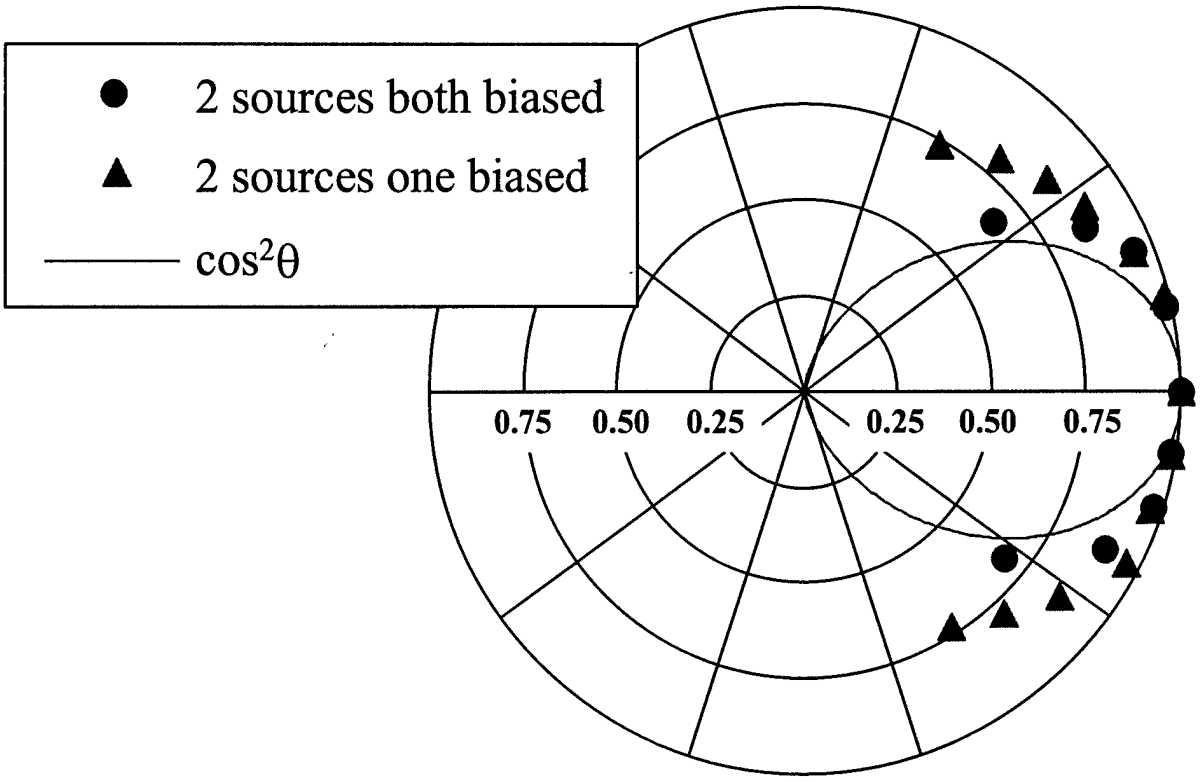

Fig. 4: Polar plot of electromagnetic radiation pattern by a single beam, dual wavelength, laser source. Two patterns are scaled to have a same bore sight gain. EM radiation beam-width narrowing was observed. The $\cos^2$ plot is shown for comparison.

Appendix II
(White Paper on LIPPES Concept)

Laser Induced, Pulsed, Picosecond, E-M Source Using a Semiconductor Antenna/Source

We propose to design, fabricate and optimize a two-element, semiconductor, photoconductive antenna/source system to demonstrate that the basic concept can be made into an efficient source/antenna element. The system is based on the concept of Laser Induced, Pulsed, Picosecond, E-M Source (LIPPES), which we have previously demonstrated at AFRL/SNHA. The advantages of the LIPPES concept are as follows; 1) when NOT illuminated (~99% of pulse cycle time), the elements are dielectric and therefore have a much lower radar cross section than conventional metallic antennae, 2) the laser excitation mechanism lends its self to optical/MEMS reconfiguring of the microwave pattern, 3) basic theory predicts that the signal strength at the source should approach the field of the bias voltage, which is on the order of thousands of volts per centimeter, 4) such system should be both simple and inexpensive suggesting increased reliability and reduced procurement and maintenance costs. A proposed budget, a description of the LIPPES concept and a summary of the research to date are presented below.

Budget

In order to optimize the efficiency of the LIPPES concept an intensified research effort will be required. If the device is to move toward a useful device, it must be assigned at least the equivalent of one fulltime researcher and some resources. At present and for the preceding two years, the level of effort for this project has been approximately 2 man months per year. This consisted of a visiting expert scientist, Dr. Everett E. Crisman, from Brown University one day per week supplemented by Dr. John Derov, AFRL/SNHA as available from his other projects. Funding recommendations; three-year, one man/per year, effort is as follows:

Fiscal Year	00	01	02
Salaries	$ 130K	$ 138K	$ 146K
Equip. & Supplies	$ 50K	$ 50K	$ 10K
Travel	$ 5K	$ 10K	$ 10K
Totals	$ 185K	$ 198K	$ 166K.

For this project, we will analyze the effects of two essential parameters necessary for efficient LIPPES operation: 1) the conversion efficiency of the radiator elements and 2) the effective isotropic power (and therefore range) of the combined radiator. The first of these tasks will be preformed by measuring the radiated E-M energy for each element as a function of both optical

excitation wavelength and the surface electric field. Using the results of that study, we will construct a model to calculate the maximum power that can be generated per element. We will than use those results to determine the design of a three dimensional array that will allow us to verify power and range predictions.

Description of Operation of LIPPES Antenna/ Source

The basic concept of the LIPPES system is shown in figure 1. The surface of slab (wafer) of semiconductor is biased with a pulse of high voltage (several thousand volts, for a microsecond) through two conducting contacts deposited on the surface at opposite edges of the slab. When a pulse of high intensity light (of duration much less than 1μsec) is incident on the surface of the semiconductor, the photo-generated, optical carriers are accelerated in the field produced by the biasing voltage. Those accelerated carriers create an electromagnetic field pulse that emulates the optical pulse.

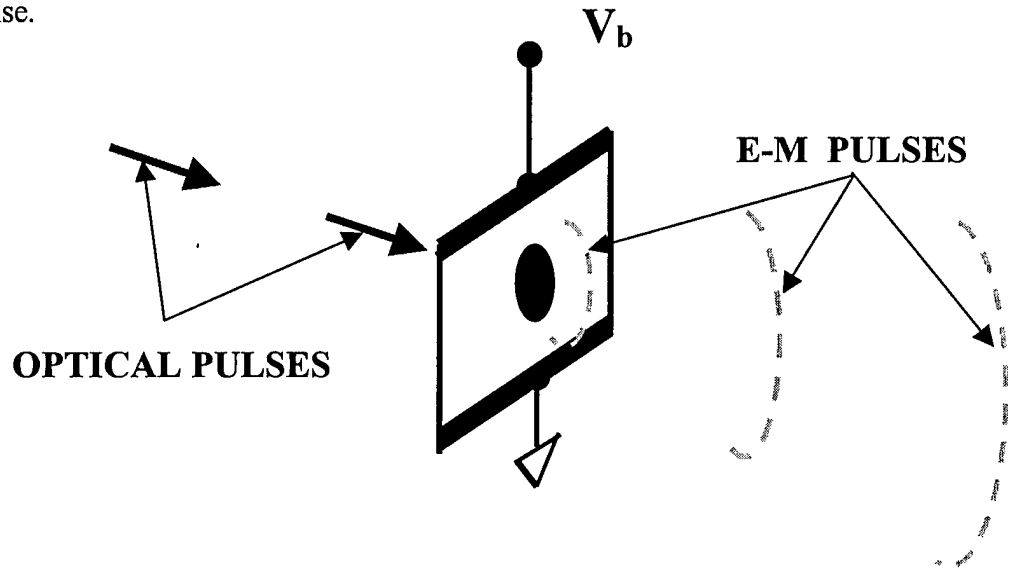

Figure 1: Schematic of the LIPPES principal.

Using conventional lasers as the light source, pulses with duration as short as femto-second can be obtained. The resulting E-M pulses will have center frequencies in the 100 THz to 100 GHz range. Calculations have shown that the corresponding bandwidths would be at least 40% of the center frequency. Using a combination of semiconductor elements in series in conjunction with illuminating multiple spots on the same element, beam intensity and steering can be controlled.

Previous Research

Briefly the LIPPES concept has been demonstrated using a mode-locked, Q-switched YLF laser system, which provided 50μJ pulse energy and 80ps pulse duration at a wavelength of 1054nm. The laser pulses were passed through a frequency doubling KDP crystal to provide 527nm pulses at a repetition rate of 378Hz. The physics of the frequency doubling process are such that significant amount of energy radiated at 1054nm passes along the optical path as well. Using a 20kV, 5μs, bias

pulse, synchronized with the laser pulse, and photo-diode triggering off a sampling oscilloscope, E-M pulses of 80ps duration were observed. (The resulting duty cycle was 0.2 percent, which means that the elements are in their dielectric state most of the time.)

A schematic of the experimental arrangement is shown in Fig. 2. A serial configuration was employed utilizing two photo-activated semiconductor elements illuminated by the dual wavelength, single laser source. Parallel excitation of multiple spots on a single semiconductor wafer element has been demonstrated also. The particular two-element system employed consisted of a GaAs wafer (closest to the laser) with an InP wafer in front. Undoped GaAs (bandgap Eg=1.43eV @RT) strongly absorbs the 527nm but is transparent at 1054nm wavelength, while the InP with Fe impurities (Eg=1.32eV @RT), absorbs significantly at 1054nm. As a result, both in-line elements are activated.

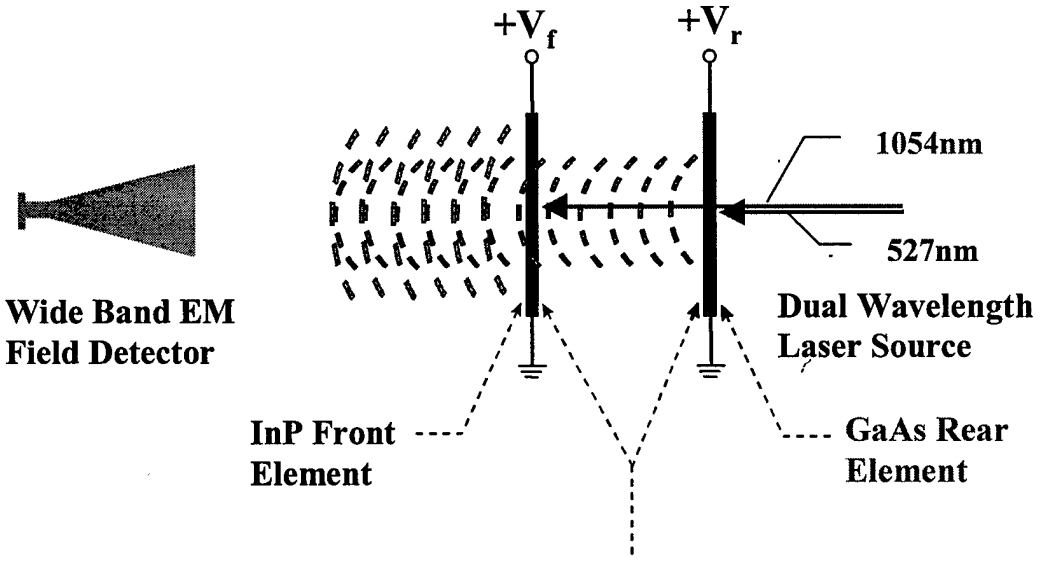

Figure 2: LIPPES configuration with a two-wavelength laser source exciting two EM radiating elements configured in series.

Traces of the E-M pulses detected from the series radiating elements are reproduced in Fig. 3. Trace (a) is the E-M pulse shape with only the front, InP, element biased with the high voltage, while trace (b) is the far field E-M pulse shape with only the rear most, GaAs, element biased. The bottom trace (c) shows the far field E-M response when both elements are biased. The oscillations to the right of the principal peaks in Fig. 2 are due to various E-M reflections (from laboratory walls, equipment, etc.) arriving at the detector after the principal event. These results demonstrate that, as theory predicts the E-M pulse from the rear element stays in phase with the laser excitation and the subsequent E-M pulse from the front element and thus the resulting far field signal is the algebraic sum of the individual element fields. Thus the output power of the source/antenna system can be

controlled by the biasing potentials on the elements, the wavelength content of the laser and/or the number of elements. We emphasize that no attempt has been made yet to optimize the LIPPES source/antenna system. Neither the choices of wavelength for the laser nor the choices of semiconductors for the elements are close to ideal. Those parameter values were, rather, an artifact of what was available or readily attainable at the time that the LIPPES concept was conceived. In addition, with the components at hand, more than 75% of the laser light is lost due to reflection at the various semiconductor surfaces. We have done some preliminary antireflection coating development, which indicates that the reflection losses can be reduced to the order of a few percent. No EM radiators have, as yet, been prepared with those AR coatings.

For the proposed project, the system will be excited by 50μJ laser pulses of 80ps duration and will, therefore, be operating in the microwave range with center frequency of 12.5GHz. Increasing the frequency to the THz range will be demonstrated using our in-house, tunable, Ti-sapphire laser that can be pulsed compressed to 1-10ps. Because the Ti-sapphire laser is tunable, we can excite the semiconductor elements near their band edge. Thus we should be able to investigate the conversion efficiency of the elements and determine the power and range limitation of such radiators. The first task will be to maximize the conversion efficiency of the radiators by measuring the output EM energy as a function of both the excitation wavelength and the quasi-dc electric field across the illuminated surface. Using those results, the second task will be to model the system in order to determine the maximum power that can be generated by each element. We should then be able to determine the design of a three dimensional array (elements excited in both parallel and series configuration) that could be used to verify our power and range predictions.

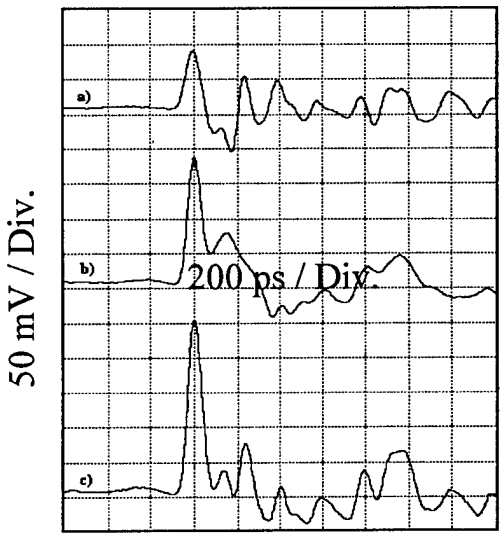

Figure. 3:
a) the EM field signal with only the front element biased, b) the EM field signal with only the rear element biased, c) the EM field signal with both elements biased.

(Note: oscillations to the right of the principal peaks are due to reflections from the lab surroundings arriving at the detector after the principal event.)

Appendix III
(White Paper on Micro-machined MM-Wave Sensors)

I Relevance

There are several military applications for MM-Wave sensors. Of particular interest the possibility of target recognition imaging. Other potential applications include unexploded ordinance recovery, land mine detection, aircraft collision avoidance and rain/fog penetration. The proposed devices require no cooling and therefore are more battle qualified than many of the competing technologies. Ready adaptation to existing Si fab-line technology implies that arrays of such sensors will be cost competitive with competing systems.

II Concept

Micro-machining is an enabling technology for millimeter wavelength sensors (30 –300 GHz). The envisioned sensor element design consists of a deposited metallic dipole antenna terminated with a thin film resistor. The dipole dimension is 'tuned' to the wavelength of the required frequency thereby absorbing energy at that wavelength. That energy is manifest as RF current that is then converted to heat in the resistor. By utilizing micro-machining techniques, the thin film terminating the resistor can be suspended above the substrate on a thin beam of silicon or silicon compound (SiO_2, Si_3N_4) thus providing thermal isolation from the substrate. Even a weak RF source will yield a significant change in resistor temperature that can be sensed with a thermopile or pryroelectric type detector. The antenna/resistor array requires somewhat complex fabrication processing but will be formed from commom metallic materials. Pyroelectric type detectors will be simple in design but are constructed from 'non-standard' materials such as GaN or AlN. The figure below is a simplified drawing of the final structure. The dipole elements per se would be of a low resistivity stable metal such as gold. The terminating resistor will be of some easily deposited compound such as Nichrome or poly-silicon. The cavity beneath the suspended resistor is formed by reactive gas etching of the sacrificial layer.

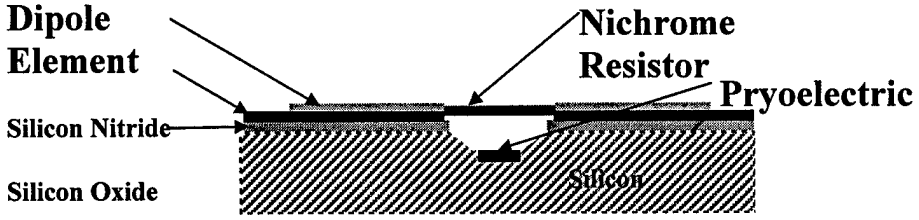

III Applications and Advantages

There are several military applications for MM-Wave sensors. Of particular interest the possibility of target recognition AND imaging (versus only tracking). Other potential applications include land mine detection, unexploded ordinance recovery, aircraft collision avoidance and rain/fog penetration. The detectors described above can be readily arrayed by combining micro-machining techniques with commercial, silicon-based integrated circuit CMOS processing. Therefore, focal plane or antenna arrays of such elements can be fabricated that include readout control circuitry. The potential for reducing the costs of arrays with this design is considerable.

VI Requested Funding

$250K is requested for this program. Details provided on request.